

# Grad-Cam Guided Progressive Feature CutMix for Classification

Yan Zhang  
452642781@qq.com  
Bin Yu He  
Li Sun

East China Normal University  
East China Normal University  
East China Normal University

## Abstract

Image features from a small local region often give strong evidence in the classification task. However, CNN suffers from paying too much attention only on these local areas, thus ignoring other discriminative regions. This paper deals with this issue by performing the attentive feature cutmix in a progressive manner, among the multi-branch classifier trained on the same task. Specifically, we build the several sequential head branches, with the first global branch fed the original features without any constraints, and other following branches given the attentive cutmix features. The grad-CAM is employed to guide input features of them, so that discriminative region blocks in the current branch are intentionally cut and replaced by those from other images, hence preventing the model from relying on only the small regions and forcing it to gradually focus on large areas. Extensive experiments have been carried out on reID datasets such as the Market1501, DukeMTMC and CUHK03, showing that the proposed algorithm can boost the classification performance significantly.

## 1 Introduction

CNN [1] has been widely adopted in the image classification and retrieval task. The large number of the parameters in CNN can be optimized by minimizing the loss functions through the stochastic gradient descent [13]. The loss function may not only reflect the classification performance like the cross entropy loss, but also evaluate the embedding distance like the center [28] or triplet loss [18]. However, some evidence [1] has shown that the CNN model actually makes the decision from only small local regions. In other words, the model seems to get satisfactory results on the given data, but it only takes advantage of very limited information, and does not perform in the reliable and explainable way, which may directly cause the over-fitting phenomena and harm the generalization performance.

Many methods and training tricks are proposed for the regularization and the further knowledge distillation in CNN. Dropout [21], dropblock [8], label smoothing [24] and smoothing temperature [10] are common ways to prevent the over-fitting and encourage the model to find more patterns in the data. On the other hand, simple data augmentations, like CutOut

[2], random erasing [33], CutMix [29, 28] are also effective particularly when the data resources are limited. However, most of these simple methods do not involve in the training loop (except [20]), and fail to model the current status of the network.

This paper proposes a simple grad-CAM guided feature CutMix method in a multi-branch classifier network for image classification. Our designed network has three sequential branches, with their input interacting with each other. The first one is provided with the original features, while the second and third one are given the different features depended on the results from its previous branch. The key idea is to progressively suppress the over highlighted spatial regions in the input feature by the CutMix operation. The results are then given to the following branch which intends to discover other patterns different from those have already been exploited. To obtain the relevant spatial regions in the current branch, we employ the grad-CAM [19] to back-propagate the correct logit score until its input. Then select the highlighted blocks and replace them with the feature blocks from other images. Note that since the grad-CAM is in the training loop, the previous branch actually affect its subsequent, making each branch focusing on different features. To verify the effectiveness of the proposed method, we carry out experiments on person re-identification (reID) task.

## 2 Backgrounds

**Person reID** is a challenging image classification task. Specifically, given a query image, the algorithms aim to find out whether the same person has appeared in the gallery, which contains a large amount of candidates who are usually recorded under a totally different view point from the queries [16]. Most large-scale reID datasets are formed with images captured in front of a market [29] or in a campus [14, 17]. Therefore, the person is often occluded by bicycles, corners, the surrounding people, etc. Sometimes, various illumination can also bring problems for reID. Overall, reID mainly suffers from the above three factors, various view angle, occlusions and volatile illumination.

In order to tackle with these difficulties, most of the recent work proposes that rather than paying too much attention on the local information, networks should explore discriminative features as much as possible. CAMA [2] constructs a three-branch structure, maximizes the differences of the class activation maps of the three branches to expand the activation area. AOS [2] blocks the input image in an adversarial way to force the network enlarge the focused area. The adversarial blocking method can only be applied offline, and require a well pre-trained person reID model. Batch DropBlock [2] performs uniform random occlusion on the feature maps of a batch image. Experimental results show that this method is simple and has good generalization.

**CAM and Grad-CAM.** Although CNN shows its great performance on computer vision, it has been criticized for its poor interpretability for a long time. The interpretability research of deep learning is then derived. The classical methods include using deconvolution and guided back propagation to visualize the features of a certain convolutional layer [20]. Such visualizations, however, cannot be used to explain the results of classification because they are not sensitive to the category and can only show all the extracted features.

Class Activation Map (CAM) [24] is a visual tool based on classification network. It connects a global average pooling layer (GAP) to the last layer of a network, transforming the feature map into a feature vector, and then a softmax is followed for classification. Each category should have a set of weights. By weighting the feature maps ( $T$ ) before GAP with the weights of a certain class, the heat map of this class ( $g$ ) can be obtained. The higher the

value is, the more the class pays attention to the region. The visualization of CAM achieves great success, but there is a drawback. The commonly used multi-layer perceptron (MLP) before the softmax has to be replaced with GAP, which usually harms the performance.

To solve this problem, Grad-CAM [19] proposes to calculate the weight ( $w$ ) by averaging the global gradient back-propagated from the score ( $\hat{y}$ ) of an interest class, which is proved to be equivalent to the weight of CAM. The detailed process is summarized in Eq 1. As it is gradient based, there is no need to change the network structure. With the perfect localization ability, CAM and grad-cam has shown their potential in fine-grained classification, weakly supervised text detection, visual question answering, etc [19, 32]. Because they are based on classification, the activated region is only determined by category, and are quite good at localization. In our work, we choose grad-CAM to guide the attentive region of our feature CutMix.

$$\begin{aligned}
 w_k &= \underbrace{\frac{1}{H \times W} \sum_{i,j}}_{\text{Global Average Pooling}} \frac{\partial \hat{y}}{\partial \mathbf{T}_{ij}^k} \\
 \mathbf{g} &= \text{ReLU} \left( \sum_k w_k \mathbf{T}^k \right)
 \end{aligned} \tag{1}$$

## 3 Proposed Method

### 3.1 Framework Overview

We use the ResNet50 [9] without down-sampling operation appended after the stage 3 as our backbone. It outputs feature maps  $\mathbf{T} \in \mathbb{R}^{H \times W \times C}$  with larger values on  $H$  and  $W$ , keeping more spatial clues in  $\mathbf{T}$ , which is also the common setting in person re-id task [1, 10, 13, 17]. As is illustrated in Figure 1, after the stage 4, our multi-branch classifier is connected, which consists of a Global branch G and two Attentive feature CutMix branch  $AC_1$  and  $AC_2$ . During the test in the image retrieval task like re-id, the final embedding vectors  $\mathbf{f}_G$ ,  $\mathbf{f}_{AC_1}$  and  $\mathbf{f}_{AC_2}$  in all branches (green cuboid in Figure 1) are concatenated to form the descriptor  $\mathbf{f}$  of a certain image. Considering the fact that a higher dimension may increase the difficulty in evaluating the embedding similarity, we intentionally control the dimension of the concatenated descriptor (e.g.,  $\mathbf{f} \in \mathbb{R}^{2048}$  in re-id).

### 3.2 Two Types of Branches.

**Global Branch G.** Similar with [2], G takes the original feature  $\mathbf{T}$  directly from the backbone, and intends mining the discriminative representations. In this branch, global average pooling (GAP) is first employed to produce the  $1 \times 1 \times C$  intermediate feature vector. Then a reduction layer, with a  $1 \times 1$  conv, BN and ReLU, is followed to further reduce the dimension of the final embedding  $\mathbf{f}_G \in \mathbb{R}^{C_G}$ , which is denoted as a green cuboid. After that, the soft-margin triplet loss  $L_{\text{triplet}}$  [10] and the softmax cross entropy loss  $L_{CE}$  are computed to make this branch to provide the global feature representations.

**Attentive CutMix Branches  $AC_1$  and  $AC_2$ .** The two branches  $AC_1$  and  $AC_2$  share their input feature maps  $\mathbf{T}'$  from the same bottleneck [8], which is the stack of conv, BN and ReLU.

This extra block is to maintain the relative independence between the branch of  $\mathbf{G}$  and the two branches of  $AC_1$  and  $AC_2$ . Therefore,  $\mathbf{T}$  and  $\mathbf{T}'$  become two different feature maps of the same dimensions.

According to the guided mask derived from grad-CAM, we are able to locate the most discriminative regions in  $\mathbf{T}$ , and replace these regions in  $\mathbf{T}'$  by features at the same location from a random sample, hence giving the mixed feature  $\mathbf{T}'_{AC_1}$  and  $\mathbf{T}'_{AC_2}$  to the two branches. This operation prevents the two inputs from highlighting the same regions as  $\mathbf{T}$ , therefore the following branch is forced to discover the new areas for the same task. The global max pooling (GMP) is then applied to the  $\mathbf{T}'_{AC_1}$  or  $\mathbf{T}'_{AC_2}$ . Similar with  $\mathbf{G}$ , the reduction layers and two loss functions are also employed in  $AC_1$  and  $AC_2$ . We denote the embedding feature vectors as  $\mathbf{f}_{AC_1}$  and  $\mathbf{f}_{AC_2}$ , respectively.

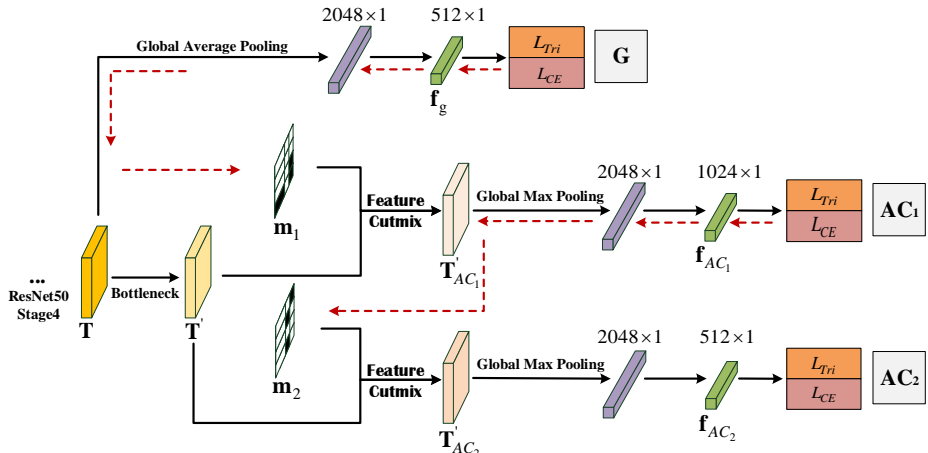


Figure 1: Overview of the proposed grad-CAM guided progressive feature CutMix scheme. For simplicity, we omit the backbone and focus on illustrating the three tail branches. The global branch  $\mathbf{G}$  is appended after the ResNet50 Stage 4. The two Attentive feature CutMix branches,  $AC_1$  and  $AC_2$ , introduce the mixed feature behind the bottleneck layer. The red dash arrows indicate the flow of the grad-CAM [10] and block ranking operation, which together generate the attentive mask to guide feature CutMix.

### 3.3 Progressive Attentive Feature Cutmix in the Multi-branch

The attentive feature CutMix are implemented under the guidance of grad-CAM in a sequential progressive way. Take the branch  $AC_1$  as an example. Given the  $\mathbf{T}$  from the backbone, we first forward propagate  $\mathbf{T}$  through the branch  $\mathbf{G}$  to obtain the classification score logits. Then only the gradients associated with the desired class are backpropagated to  $\mathbf{T}$ , which is then combined to generate a one channel grad-CAM feature map  $\mathbf{g} \in \mathbb{R}^{H \times W}$ . Thus the binarized mask  $\mathbf{m}$ , with the same spatial dimensions as  $\mathbf{g}$ , guides the feature CutMix for the  $AC_1$  branch. Although two branches of  $\mathbf{G}$  and  $AC_1$  are connected by  $\mathbf{m}$ , gradients in  $AC_1$  are supposed to be stopped on it, making sure the independence of them. Similarly, the grad-CAM feature  $\mathbf{g}$  from  $AC_1$  further guides the CutMix operation in  $AC_2$ . Notice that, the binary

masks  $\mathbf{m}$  are combined with the original feature  $\mathbf{T}'$ , giving mixed features  $\mathbf{T}'_{AC_1}$  and  $\mathbf{T}'_{AC_2}$  as the inputs for  $AC_1$  and  $AC_2$  branches, respectively. Hence, the more discriminative regions can be found by these two CutMix branches, which progressively enlarges the relevant areas for the classification task.

Figure 2 shows the whole procedure of the proposed Attentive Feature CutMix. The grad-CAM results  $\mathbf{g}$ , generated from the upper global branch G first turns into a binary mask  $\mathbf{m}$  through the block ranking operation. Then, according to  $\mathbf{m}$ , a given anchor feature map  $\mathbf{T}'_A$  is to be cut and mixed with a  $\mathbf{T}'_N$  from another image. We now illustrate the block ranking and feature CutMix operations in following two subsections.

**The Block Ranking.** A grad-CAM features  $\mathbf{g}$ , computed from the gradients, is supposed to be spilt into the several blocks with the fixed size, denoted as  $\mathbf{b}_i \in \mathbb{R}^{b_h \times b_w}$ ,  $i$  is the index of the block,  $b_h$  and  $b_w$  are the height and width of all the blocks. We specify that the width  $W$  and height  $H$  of  $\mathbf{g}$  should be an integer multiple of  $b_w$  and  $b_h$ , respectively. And there is no overlap between two adjacent blocks. Then,  $\mathbf{b}_i$  are summed into a scalar  $e_i$  to provide the ranking evidence of the  $i$ th block. Obviously, the higher value of  $e_i$  indicates that the block  $\mathbf{b}_i$  contributes a lot in the current classification branch, and following branches are intentionally designed for finding other regions. According to the ranking result, the top  $k$  blocks in  $\mathbf{m}$  are to be zeroed out, while others are set as one, as is shown in following equation.  $j \in [1, H \times W]$  is the index on the spatial dimension of the generated mask.

$$\mathbf{m}_j = \begin{cases} 0 & j \in \{b_i\} \& e_i \in \{top_k(e)\} \\ 1 & others \end{cases} \quad (2)$$

**Feature CutMix.** The goal is to generate the combined features by  $\mathbf{T}'_A$  and  $\mathbf{T}'_N$  from two images. Here the subscript  $A$  indicates an anchor feature, and  $N$  represents the negative sample of the anchor. Compared with selecting a random sample to do the CutMix, which is proposed in [28], mixed with a random negative feature shows better performance. The related discussions are listed in Table 4. The CutMix operation is summarized in Eq. 3. Here  $\odot$  indicates the spatial multiplication between the single channel mask  $\mathbf{m}$  and the  $C$  channels feature maps. The result  $\mathbf{T}'_{AC}$  is used as the input for two branches, either the  $\mathbf{T}'_{AC_1}$  or  $\mathbf{T}'_{AC_2}$ .

$$\mathbf{T}'_{AC} = \mathbf{m} \odot \mathbf{T}'_A + (1 - \mathbf{m}) \odot \mathbf{T}'_N \quad (3)$$

## 4 Experiments

### 4.1 Datasets and Evaluation Metrics

We evaluate our proposed methods on three generally used person re-ID benchmarks, including Market-1501 [29], DukeMTMC-reID [30] and CUHK03[31]. **Market-1501** [29] contains large-scale images captured from 6 different cameras, 5 of which is of high-resolution, and one is a low-resolution camera. The annotated bounding boxes are automatically obtained by Deformable Part Model (DPM) [32]. Therefore, in addition to the positive bounding boxes, the false alarm samples are also provided. Overall, this dataset consists of 32,668 images of 1,501 identities, and each identity is present in at least 2 camera-views.

**DukeMTMC-reID** [30] contains 36,411 images taken from 8 high-resolution cameras, with manual annotations. In this dataset, a total of 1,404 identities appear under more than

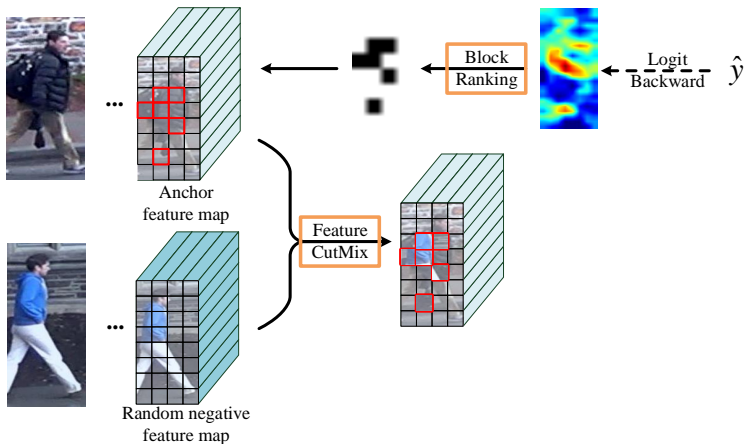


Figure 2: The whole process of the attentive feature CutMix. We divide it into two steps, *i.e.* the block ranking step and the feature CutMix step. Firstly, taking a grad-CAM, corresponding to the expected class, the block ranking operation turns it into a binary block mask (0 for the highlighted regions in grad-CAM and 1 for others). Then, according to the binary mask, the highlighted regions of an anchor feature map will be replaced by the corresponding region features from a random negative feature map in the feature CutMix step.

two cameras, and 408 identities appear under only one camera. The standard evaluation protocol evenly splits the 1,404 identities into the training and the testing set. The remained 408 identities are used as interference items, and are added into the gallery.

In **CUHK03** [14], 13,164 images of 1,360 identities are included. These images are recorded by 6 surveillance cameras, and each identity is observed by two non-overlapped cameras. Both the manually annotated version and the DPM annotated one are provided, namely CUHK03-Label and CUHK03-Detect. Note that, we apply the new partition method of CUHK03, which is of the same format with the Market-1501 and the DukeMTMC-reID.

The standard strategy of the above datasets for generating the training set, gallery and the query is listed in Table 4.1. The identities in training set and the test set are supposed to be non-overlap, so do the images in the gallery and the query. As is shown in Table 4.1, CUHK03 possesses the least training samples, which makes it become the most challenging dataset among the three.

For evaluation, we choose the Euclidean distance between each query images and all the gallery images as the similarity measurement, and compute the Cumulative Matching Characteristic (CMC) curve [8]. The evaluation metrics we adopted are Rank-1 accuracy and mean average precision (mAP) [29]. Notice that, all the provided results are without re-ranking [32].

## 4.2 Implementation Details

During training, all the input images are resized to  $384 \times 128$ , and then are augmented by random horizontal flip, normalization and Cutout [10]. In the feature CutMix layer, We fix the size of the every single cell as  $3 \times 2$ , and we set the number of mixed cell per anchor as

**Table 1: Detailed partition statistics of the classic person reID datasets.**

Dataset	Training Set		Test Set			
			Gallery		Query	
	#ID	#Images	#ID	#Images	#ID	#Images
Market-1501	751	12,936	750	19,732	750	3,368
DukeMTMC-reID	702	16,522	1,110	17,661	702	2,228
CUHK03-Labeled	767	7,368	700	5,328	700	1,400
CUHK03-Detected	767	7,365	700	5,332	700	1,400

6, which is applied to all the evaluated datasets. During the test phase, the input images are resized to  $384 \times 128$  and then just augmented by normalization. Feature CutMix operation is omitted in this phase.

Our work is trained on a single GTX1080Ti GPU with a batch size of 64. Each identity contains 4 instances, *i.e.* there are 16 identities per batch. The backbone network is initialized with the ImageNet [3] pretrained ResNet50. We use batch hard triplet loss with soft margin [10], thus we do not need to tune the margin hyper-parameter. A total of the training epoch is 500 for all datasets. We use Adam optimizer with the base learning rate as 1e-3 with a linear warm-up [9] in the first 50 epochs, then it is decayed by 10 at 200 and 300 epoch.

## 4.3 Results and Analysis

### 4.3.1 Comparison with State-of-the-Art

The comparison results between our proposition and the state-of-the-art methods on CUHK03, DukeMTMC-reID and Market-1501 datasets are listed in Table 4.3.1. To be fair, we train BDB [2] with batch size 64, and the results is notated as **BDB\***. The claimed results in [2] are listed in line **BDB** as a contrast. Compared with the BDB network, our method contains one more branch. So we extend the original BDB network to a three-branch structure, which is almost the same with our framework ( Figure 1 ) but the two grad-CAM guided feature CutMix operation is replaced with two independent Batch DropBlocks [2]. This model is notated as **BDB\*3**. As is shown in Table 4.3.1, our method has achieved great improvement compared with the previous work, especially for CUHK03 dataset, which is the most challenging one among the three. Under the same batch size setting, our method can get competitive performance with the BDB\* and BDB\*3. Furthermore, our method shows great potential on CUHK03, the mAP on CUHK03-Detected even exceeds the BDB network trained with batch size 128.

### 4.3.2 Ablation Studies

In this section, extensive experiments are conducted on DukeMTMC-reID and CUHK03-Detected to analyse the effectiveness of the proposed components and the impact of the related hyper-parameters.

**Benefit of Global branch and Progressive Feature CutMix Branch.** Table 4.3.2 lists the evaluation results of different combinations of branches. On the basis of **G** ( a single global branch ), adding two independent Batch DropBlocks sequentially greatly improves the performance. For CUHK03, on the basis of **G**, only adding one feature CutMix branch can make 0.3% increase on mAP, compared with **BDB\*3**. Then the addition of one more feature

Table 2: Comparison results with the state-of-the-art methods on the classic person reID datasets.

Methods	CUHK03-Labeled		CUHK03-Detected		DukeMTMC-reID		Market-1501	
	Rank-1	mAP	Rank-1	mAP	Rank-1	mAP	Rank-1	mAP
IDE [20]	22.2	21.0	21.3	19.7	67.7	47.1	72.5	46.0
PAN [20]	36.9	35.0	36.3	34.0	71.6	51.5	82.8	63.4
SDVNet [20]	-	-	41.5	37.3	76.7	56.8	82.3	62.1
HA-CNN [20]	44.4	80.0	88.7	77.8	85.2	72.8	62.9	51.5
SVDNet+Era [20]	49.4	45.0	48.7	37.2	79.3	62.4	87.1	71.3
TriNet+Era [20]	58.1	53.8	55.5	50.7	73.0	56.6	83.9	68.7
AOS [20]	-	-	54.6	56.1	79.2	62.1	91.3	78.3
PCB [20]	-	-	61.3	54.2	81.9	65.3	92.4	77.3
PCB+RPP [20]	-	-	62.8	56.7	83.3	69.2	93.8	81.6
CAMA [20]	70.1	66.5	66.6	64.2	85.8	72.9	94.7	84.5
BDB* [20]	76.6	73.2	72.4	69.5	87.7	74.5	94.0	84.9
BDB*3	77.3	74.5	74.3	71.2	<b>88.2</b>	<b>74.9</b>	94.3	84.9
Ours	<b>78.4</b>	<b>75.4</b>	<b>75.2</b>	<b>73.6</b>	88.0	74.6	<b>94.5</b>	<b>85.2</b>

Table 3: Benefit of Global branch and Progressive Feature CutMix Branch on CUHK03-Detected and DukeMTMC-reID.

Branch	CUHK03-Detected		DukeMTMC-reID	
	Rank1	mAP	Rank1	mAP
G	65.1	60.1	83.8	68.6
+ BDB1 ( BDB* )	72.4	69.5	87.1	74.5
+ BDB2 ( BDB*3 )	74.3	71.2	<b>88.3</b>	<b>74.7</b>
+ PC1	74.1	71.5	86.4	73.0
+ PC2	<b>75.4</b>	<b>73.0</b>	88.0	74.6

CutMix branch further brings another 1.3% and 2.5% increase on Rank1 and mAP, respectively. Although the two feature CutMix branches cannot exceed the **BDB\*** and **BDB\*3**, they can still achieve competitive performance. The motivation behind the three-branch structure is that an extra branch with a different interference mode provides complementary clues. In addition, our feature CutMix is grad-CAM guided. By progressively applying the attentive feature CutMix, the most discriminative features are to be replaced by interference, which forces the whole network to exploit more fine-grained discriminative features.

**Impact of Different Sampling ways.** There are three ways to implement feature CutMix, *i.e.* sampling interference from positive pairs, from negative pairs, or from both. The test results are shown in Table 4. As for Rank1, different sampling methods make little difference, while for mAP, the negative sampling brings 1.5% increase, compared with the poorest positive sampling. This is reasonable, as the negative sampling introduces the hardest interference, which is due to make the model more robust.

Table 4: Impact of different sampling ways in feature CutMix on DukeMTMC-reID. **P** means sample from positive pairs, **P+N** is to randomly sample from a batch, and **N** refers to sampling only from negative pairs in a batch.

Methods	CUHK03-Detected		DukeMTMC-reID	
	Rank-1	mAP	Rank-1	mAP
P	70.1	66.4	86.7	72.0
P+N	74.9	71.1	<b>87.1</b>	72.8
N	<b>75.0</b>	<b>71.8</b>	86.9	<b>73.5</b>

**Impact of the Hyper-parameter in Feature CutMix.** Figure 3 illustrates the impact of different hyper-parameter  $K$  in CutMix on the performance. The increase in  $k$  means the increase of areas of interference. As we can see in Figure 3, the best performance gets to the peak at  $k$  equals 8, which is then fixed for all experiments on CUHK03 dataset. According to our settings, when  $k$  gets to 8, the total cutmixed area is one third of the whole feature map, which equals to the setting of BDB [2], but our approach provides more flexible and orientated interference. It worth noticing that the  $k$  can be slightly different for various datasets. As for DukeMTMC-reID and Market-1501, the  $k$  is fixed as 6.



Figure 3: The impact of hyper-parameter  $k$  in feature CutMix. The statistics are analyzes on the CUHK03-Detected dataset.

**Effectiveness of Each Branch.** The visualization of the grad-CAM of branch  $G$ ,  $AC_1$  and  $AC_2$  are illustrated in Figure 4. We can see that the activation map learned by the three branches are different from each other, thus they can mutually provide complementary information. It is evident that, by blocking the highlighted regions, we can reinforce the response of features from the rest parts.

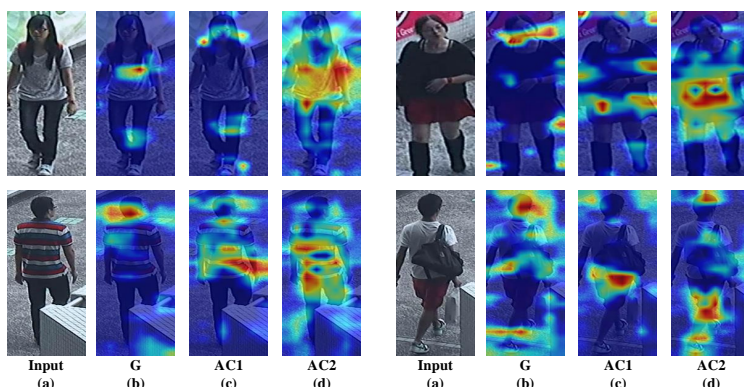


Figure 4: The grad-CAM of each branch of our network. The visualization is conducted on CUHK03-Detected.

## 5 Conclusion

## References

- [1] Wieland Brendel and Matthias Bethge. Approximating cnns with bag-of-local-features models works surprisingly well on imagenet. *arXiv preprint arXiv:1904.00760*, 2019.
- [2] Zuozhuo Dai, Mingqiang Chen, Xiaodong Gu, Siyu Zhu, and Ping Tan. Batch drop-block network for person re-identification and beyond. In *Proceedings of the IEEE International Conference on Computer Vision*, pages 3691–3701, 2019.
- [3] Jia Deng, Wei Dong, Richard Socher, Li-Jia Li, Kai Li, and Li Fei-Fei. Imagenet: A large-scale hierarchical image database. In *2009 IEEE conference on computer vision and pattern recognition*, pages 248–255. Ieee, 2009.
- [4] Terrance DeVries and Graham W Taylor. Improved regularization of convolutional neural networks with cutout. *arXiv preprint arXiv:1708.04552*, 2017.
- [5] Pedro F Felzenszwalb, Ross B Girshick, David McAllester, and Deva Ramanan. Object detection with discriminatively trained part-based models. *IEEE transactions on pattern analysis and machine intelligence*, 32(9):1627–1645, 2009.
- [6] Golnaz Ghiasi, Tsung-Yi Lin, and Quoc V Le. Dropblock: A regularization method for convolutional networks. In *Advances in Neural Information Processing Systems*, pages 10727–10737, 2018.
- [7] Priya Goyal, Piotr Dollár, Ross Girshick, Pieter Noordhuis, Lukasz Wesolowski, Aapo Kyrola, Andrew Tulloch, Yangqing Jia, and Kaiming He. Accurate, large minibatch sgd: Training imagenet in 1 hour. *arXiv preprint arXiv:1706.02677*, 2017.
- [8] Douglas Gray, Shane Brennan, and Hai Tao. Evaluating appearance models for recognition, reacquisition, and tracking. In *Proc. IEEE international workshop on performance evaluation for tracking and surveillance (PETS)*, volume 3, pages 1–7. Citeseer, 2007.
- [9] Kaiming He, Xiangyu Zhang, Shaoqing Ren, and Jian Sun. Deep residual learning for image recognition. In *Proceedings of the IEEE conference on computer vision and pattern recognition*, pages 770–778, 2016.
- [10] Alexander Hermans, Lucas Beyer, and Bastian Leibe. In defense of the triplet loss for person re-identification. *arXiv preprint arXiv:1703.07737*, 2017.
- [11] Geoffrey Hinton, Oriol Vinyals, and Jeff Dean. Distilling the knowledge in a neural network. *arXiv preprint arXiv:1503.02531*, 2015.
- [12] Houjing Huang, Dangwei Li, Zhang Zhang, Xiaotang Chen, and Kaiqi Huang. Adversarially occluded samples for person re-identification. In *Proceedings of the IEEE Conference on Computer Vision and Pattern Recognition*, pages 5098–5107, 2018.
- [13] Diederik P Kingma and Jimmy Ba. Adam: A method for stochastic optimization. *arXiv preprint arXiv:1412.6980*, 2014.

- [14] Wei Li, Rui Zhao, Tong Xiao, and Xiaogang Wang. Deepreid: Deep filter pairing neural network for person re-identification. In *Proceedings of the IEEE conference on computer vision and pattern recognition*, pages 152–159, 2014.
- [15] Wei Li, Xiatian Zhu, and Shaogang Gong. Harmonious attention network for person re-identification. In *Proceedings of the IEEE conference on computer vision and pattern recognition*, pages 2285–2294, 2018.
- [16] Xiang Li, Ancong Wu, and Wei-Shi Zheng. Adversarial open-world person re-identification. In *Proceedings of the European Conference on Computer Vision (ECCV)*, pages 280–296, 2018.
- [17] Ergys Ristani, Francesco Solera, Roger Zou, Rita Cucchiara, and Carlo Tomasi. Performance measures and a data set for multi-target, multi-camera tracking. In *European Conference on Computer Vision*, pages 17–35. Springer, 2016.
- [18] Florian Schroff, Dmitry Kalenichenko, and James Philbin. Facenet: A unified embedding for face recognition and clustering. In *Proceedings of the IEEE conference on computer vision and pattern recognition*, pages 815–823, 2015.
- [19] Ramprasaath R. Selvaraju, Abhishek Das, Ramakrishna Vedantam, Michael Cogswell, Devi Parikh, and Dhruv Batra. Grad-cam: Why did you say that? visual explanations from deep networks via gradient-based localization. *CoRR*, abs/1610.02391, 2016. URL <http://arxiv.org/abs/1610.02391>.
- [20] Jost Tobias Springenberg, Alexey Dosovitskiy, Thomas Brox, and Martin Riedmiller. Striving for simplicity: The all convolutional net. *arXiv preprint arXiv:1412.6806*, 2014.
- [21] Nitish Srivastava, Geoffrey Hinton, Alex Krizhevsky, Ilya Sutskever, and Ruslan Salakhutdinov. Dropout: a simple way to prevent neural networks from overfitting. *The journal of machine learning research*, 15(1):1929–1958, 2014.
- [22] Yifan Sun, Liang Zheng, Weijian Deng, and Shengjin Wang. Svdnet for pedestrian retrieval. In *Proceedings of the IEEE International Conference on Computer Vision*, pages 3800–3808, 2017.
- [23] Yifan Sun, Liang Zheng, Yi Yang, Qi Tian, and Shengjin Wang. Beyond part models: Person retrieval with refined part pooling (and a strong convolutional baseline). In *Proceedings of the European Conference on Computer Vision (ECCV)*, pages 480–496, 2018.
- [24] Christian Szegedy, Vincent Vanhoucke, Sergey Ioffe, Jon Shlens, and Zbigniew Wojna. Rethinking the inception architecture for computer vision. In *Proceedings of the IEEE conference on computer vision and pattern recognition*, pages 2818–2826, 2016.
- [25] Devesh Walawalkar, Zhiqiang Shen, Zechun Liu, and Marios Savvides. Attentive cutmix: An enhanced data augmentation approach for deep learning based image classification. *arXiv preprint arXiv:2003.13048*, 2020.
- [26] Yandong Wen, Kaipeng Zhang, Zhifeng Li, and Yu Qiao. A discriminative feature learning approach for deep face recognition. In *European conference on computer vision*, pages 499–515. Springer, 2016.

- [27] Wenjie Yang, Houjing Huang, Zhang Zhang, Xiaotang Chen, Kaiqi Huang, and Shu Zhang. Towards rich feature discovery with class activation maps augmentation for person re-identification. In *Proceedings of the IEEE Conference on Computer Vision and Pattern Recognition*, pages 1389–1398, 2019.
- [28] Sangdoo Yun, Dongyoon Han, Seong Joon Oh, Sanghyuk Chun, Junsuk Choe, and Youngjoon Yoo. Cutmix: Regularization strategy to train strong classifiers with localizable features. In *Proceedings of the IEEE International Conference on Computer Vision*, pages 6023–6032, 2019.
- [29] Liang Zheng, Liyue Shen, Lu Tian, Shengjin Wang, Jingdong Wang, and Qi Tian. Scalable person re-identification: A benchmark. In *Computer Vision, IEEE International Conference on*, 2015.
- [30] Liang Zheng, Yi Yang, and Alexander G Hauptmann. Person re-identification: Past, present and future. *arXiv preprint arXiv:1610.02984*, 2016.
- [31] Zhedong Zheng, Liang Zheng, and Yi Yang. Pedestrian alignment network for large-scale person re-identification. *IEEE Transactions on Circuits and Systems for Video Technology*, 29(10):3037–3045, 2018.
- [32] Zhun Zhong, Liang Zheng, Donglin Cao, and Shaozi Li. Re-ranking person re-identification with k-reciprocal encoding. In *CVPR*, 2017.
- [33] Zhun Zhong, Liang Zheng, Guoliang Kang, Shaozi Li, and Yi Yang. Random erasing data augmentation. *arXiv preprint arXiv:1708.04896*, 2017.
- [34] Bolei Zhou, Aditya Khosla, Agata Lapedriza, Aude Oliva, and Antonio Torralba. Learning deep features for discriminative localization. In *Proceedings of the IEEE conference on computer vision and pattern recognition*, pages 2921–2929, 2016.